GEOLOGICAL EXPLORATION OF SOUTHERN UTOPIA PLANITIA BY TIANWEN-1 ZHURONG ROVER.

Yang Steve Liu[1], Yuyan Sara Zhao[2], Lu Pan[3], Zongcheng Ling[4], Ling Chen[5], and Yongliao Zou[1], [1]National Space Science Center, Chinese Academy of Sciences, Beijing 100190, China (yangliu@nssc.ac.cn). [2]College of Earth Science, Chengdu University of Technology, Chengdu 610059, China. [3]School of Earth and Space Sciences, University of Science and Technology of China, Hefei 230026, China. [4]School of Space Science and Physics, Institute of Space Sciences, Shandong University, 264209, Weihai, China. [5]Institute of Geology and Geophysics, Chinese Academy of Sciences, Beijing 100029, China.

Introduction: The Tianwen-1 Mars mission successfully landed the Zhurong rover in the southern Utopia Planitia at 25.066°N, 109.925°E in 2020 [1] (Fig. 1). The rover is equipped with six scientific payloads, including Navigation and Terrain camera (NaTeCam), Mars Rover Magnetometer (RoMAG), Multispectral Camera (MSCam), Mars Climate Station-1&2 (MSC-1: Wind field and sound probe; MSC-2: Air temperature and pressure probe), Mars Surface Component Detector (MarSCoDe), and Mars Rover Penetrating Radar (RoPeR: channel 1 and 2). The main objectives of the Zhurong rover are to investigate the morphology, mineralogy, space environment, subsurface structure, and water/ice distribution of the southern Utopia Planitia [2,3]. Until Sept 4, 2021, the Zhurong rover has completed its nominal exploration period for 92 sols. The rover has traversed 1,921 m until May 18, 2022 when the rover entered the hibernation mode. Here we report the recent scientific results of the geological exploration of the Utopia Planitia by Zhurong rover.

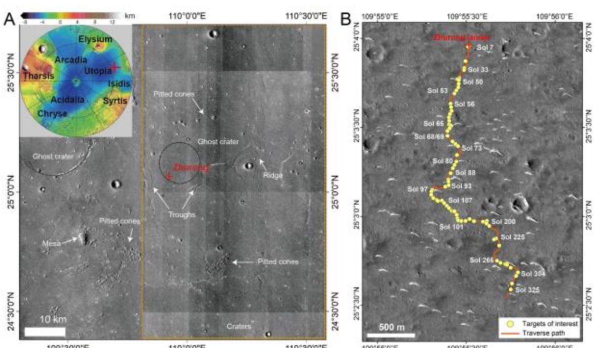

Fig. 1. Geological context and traverse of Zhurong rover

Geomorphology: The terrain Zhurong traversed is smooth with a few rocks and resolvable granules and pebbles in the NaTeCam images, mainly composed of sand-sized particles ranging between 500 μm to 2 mm consistent with the thermal inertia values of 250-350 $JK^{-1}m^{-2}s^{-1/2}$ [4]. Clustered, embedded, and buried rocks are all observed modulated by the impact process and the removal or deposition of fine-grained sands. Two distinct types of rocks were observed. One dark-toned rock group often is exposed in the far-field, with predominantly angular shapes and varying sizes. Some of these dark-toned rocks show vesicular surfaces. Since the dark-toned rocks often distribute on the rim of small buried impact craters, they are interpreted as excavated basaltic rocks. On the other hand, bright-toned rocks in the NaTeCam images, ranging from 8 to 18 cm in size, are scattered on the ground in clustered patches. These rocks often are covered by dust and soils and show flaking or peeling surfaces suggesting physical weathering by thermal stress and aeolian processes. Some of these bright rocks with light-toned rinds have dark interiors that is distinctive from these flaking rocks. We identify several small, simple craters surrounded by ejected fragments, and sometimes entirely buried by fines. Aeolian bedforms (e.g., dunes or ripples) are common in the landing areas, covered by both bright and dark sands on the surface.

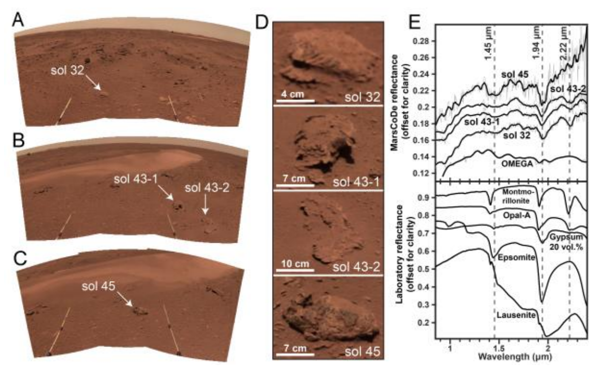

Fig. 2. Targets of interest and VNIR spectra

VNIR spectral analysis: Short Wave Infrared (SWIR) spectral data in the visible and near infrared (VNIR) wavelength range over the rocks obtained by the Zhurong rover show a distinct asymmetric 1.93-1.95 μm absorption feature and an additional absorption around 2.22 μm (Fig. 2). The observed major spectral features could be explained by hydrated silica or hydrated sulfates. However, the low signal-to-noise ratio and the absence of other diagnostic features preclude an unambiguous mineral identification. From sol 24 onwards, the Zhurong rover has continuously observed planar rock flats, some in perched position and slightly above the ground. These rock slabs are light-toned, have irregular and rough surfaces, and show significantly different morphology and macrotexture from the dark-toned basalts at this site or pristine basalts at previous landing sites on Mars. They are also distinctive from those bright rocks with dark interiors but light-toned rinds. The platy rocks are generally resistant to deflation and therefore preserved with a fine-layered structure due to physical weathering. We interpret these bright-toned rocks to be a layer of locally developed duricrust. In this case, the pre-depositional regolith underwent cementation and lithification during the rising or infiltration of briny groundwater to form the observed platy rocks [5].

LIBS analysis: We investigated the aqueous alteration of the rock and soils encountered by Zhurong rover in the first 300 sols. Major elemental abundance is derived through the Laser-Induced Breakdown Spectrometer (LIBS) dataset acquired by the Mars Surface Composition Detector (MarSCoDe). The results show that most materials at the Tianwen-1 landing site have low Chemical Index of Alteration (CIA) values (< 39%±9%) based on the LIBS spectra. We find that the fine-grained soil at the Tianwen-1 landing site is very similar to the ubiquitous surface dust at other landing sites on Mars. Rock and soils met by Zhurong rover are mostly igneous basaltic materials mixed with secondary minerals and they appear to have a low degree of chemical alteration [6].

Subsurface structure: An in-situ ground-penetrating radar survey of southern Utopia Planitia conducted by the Zhurong rover of the Tianwen-1 mission. A detailed subsurface image profile is constructed, revealing a ~70-m thick, multi-layered structure below a <10-m thick regolith. The new radar image suggests the possible occurrence of episodic hydraulic sedimentation that is interpreted to represent the basin infilling of Utopia Planitia during the Late Hesperian to Middle Amazonian epochs [7].

Aeolian bedforms: A large amount of transverse aeolian ridges (TAR) bedforms exist in the Zhurong rover landing region. The acquisition of high-resolution data from obiter and the rover from Tianwen-1 mission provide an excellent opportunity to study the geological characteristics of TARs. We identity and analyze a total of 8,274 TAR samples, and the results show that the length and width of TARs in the study region range between 7.3-329 m and between 1.6-54 m, respectively. The orientations of TARs are shown in the rose diagram (Fig. 3). It is found that E-W is the average dominant orientation and ESE-WNW is the secondarily dominant orientation for all the TAR samples. According to the Zhurong rover MCS data, SSW is the main wind regime direction of Martian present-day climate, and the SW is the secondary direction (Fig. 3). The age of these TARs is also analyzed. According to the spatial relationship between TARs and craters, the craters surrounded and overlaid on TARs, respectively, were extracted using the CraterTools. The ages of these two types of craters were used to constrain the upper and lower limits of the TARs formation and development, which varies from 64^{+20}_{-20} ka to 260^{+30}_{-30} Ma. TARs have dust-covered surfaces, implying that the ripples may be inactive. These results have important implications on the aeolian processes and climate evolution on Mars.

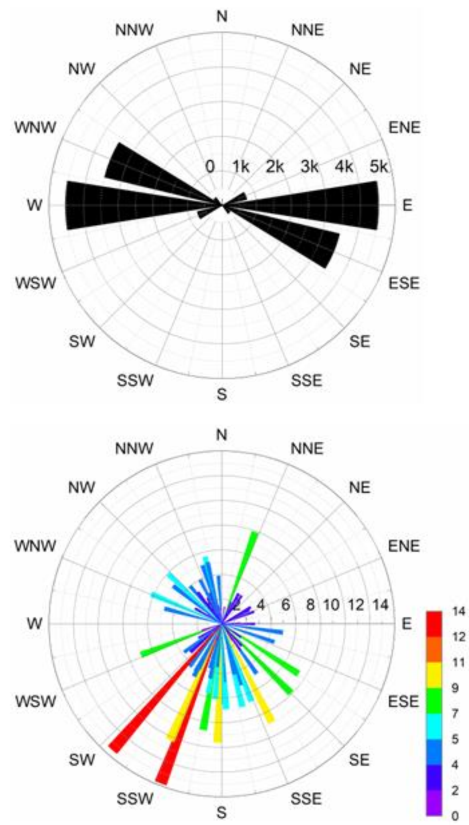

Fig. 3. The orientation of TARs (uppper) and local wind direction (bottom)

Acknowledgments: We are grateful to the Tianwen-1 engineering team for such a successful mission, payload team for mission operations, and China National Space Administration (CNSA) for providing the Tianwen-1 scientific data that made this study possible. This data set is processed and produced by Ground Research and Application System (GRAS) of China's Lunar and Planetary Exploration Program, provided by China National Space Administration (http://moon.bao.ac.cn).

References:

[1] J. Liu et al.(2021), Nat. Astron. [2] W. X. Wan et al. (2020), Nat. Astron. 4, 721-721. [3] Y. Zou et al. (2021), Adv. Space Res. 67, 812-823. [4] M. A. Presley, P. R. Christensen (1997), J. Geophys. Res. 102, 6535-6549. [5] Y. Liu et al. (2022), Science Advances, 8, eabn8555. [6] Q. Liu et al. (2022), Communications Earth & Environment volume 3, 280. [7] Li et al. (2022), Nature, 610.